Tribology International 160 (2021) 107001

Contents lists available at ScienceDirect

Tribology International

journal homepage: http://www.elsevier.com/locate/triboint

Method for tribological experiment to study scuffing initiation on AISI 52100 steel and hard ceramic coatings

Kelly Jacques [a,b], Nikhil Murthy [b], Satish Dixit [c], Diana Berman [a,*], Stephen Berkebile [b,**]

[a] Materials Science and Engineering, University of North Texas, Denton, TX, 76203, USA
[b] Vehicle Technology Directorate, U.S. CCDC Army Research Laboratory, 6340 Rodman Road, Aberdeen Proving Ground, MD, 21005, USA
[c] Plasma Technology Inc., Torrance, CA, 90501, USA

ARTICLE INFO

Keywords:
Scuffing
Wear-resistance
Hard coatings
Low viscosity fuels

ABSTRACT

Though many models of wear have been proposed, the design of the lab-scale experimental procedures to reproduce and characterize a particular wear regime, scuffing, has been difficult to generalize and more limited in scope. In this study, we used a high-frequency reciprocating tribometer to determine a set of tribological experimental parameters that instigate material scuffing and yield reliable and repeatable results by varying grinding lay orientation, temperature, counter body material, substrate hardness, contact load, stroke length, and frequency. The onset of scuffing in through-hardened 52100 steel substrates lubricated with low viscosity fuels was most repeatable with a perpendicular grinding lay and alumina counterface, while no effect was observed with substrate temperature. The experimental method using a load progression from 1 N to 18 N was then used on several protective coatings to determine their effectiveness in inhibiting scuffing initiation.

1. Introduction

One of the most detrimental challenges facing mechanical components is tribologically-induced damage and wear of contacting surfaces [1]. Among different wear mechanisms, specific research interest is attributed to the tribological phenomenon called scuffing [2] due to its catastrophic consequences leading to failure of mechanical systems, such as fuel systems in combustion engines. While the phenomenon of scuffing is not fully understood, its origin is usually attributed to insufficient lubrication under extreme load and speed conditions, leading to high friction, heat generation, adhesion, and oxidation between the sliding surfaces.

Previously, several different models to explain scuffing were proposed [2]. The major role in those models is usually attributed to the contact temperature increase. Specifically, Blok [3,4] suggested that scuffing is initiated when the contact temperature reaches some critical value associated with the instantaneous "flash temperature" rise in the sliding asperities. The contact temperature increase is largely affected by the sliding conditions, viscosity and chemistry of the liquid lubricant, and the roughness and thermal properties of the contacting surfaces. The number of those contacting asperities experiencing a flash temperature increase largely affected the degree of scuffing [5,6]. While in the standard flash temperature model the lubricant was mostly considered as a third body affecting friction and heat dissipation in the contact [7,8], later models suggested that scuffing originates upon the breakdown of the elastohydrodynamic lubrication (EHL) film when reaching a critical temperature leading to sudden lubricant viscosity change [9]. In case of the mixed and boundary lubrication regimes, the role of the lubricant viscosity was suppressed and more effect was attributed to the dominance of the lubricant desorption [10] or even decomposition [2] upon heating of the sliding surfaces resulting in the loss of lubrication and leading to the higher friction regime. In all the mentioned scuffing models, insufficient lubrication eventually led to the direct asperity interactions and plastic flow of the materials in contact [11]. Large-scale, rapid wear of the material occurred as a result of the scuffing, and the process was affected by non-uniformity across the surface of a material, lubrication regime, surface finish, and material characteristics [12]. To further understanding of the effect of surface contact and sliding conditions on scuffing, experimental efforts have been directed towards reaching the scuffing regimes in lab-scale settings. The key parameters that were considered in such studies are the effects of the environment, grinding lay orientation, surface roughness, and specimen materials

* Corresponding author.
** Corresponding author.
E-mail addresses: diana.berman@unt.edu (D. Berman), stephen.p.berkebile.civ@mail.mil (S. Berkebile).

https://doi.org/10.1016/j.triboint.2021.107001
Received 29 October 2020; Received in revised form 2 March 2021; Accepted 14 March 2021
Available online 24 March 2021

Table 1
Experimental parameters for investigations.

Investigation	Counter Body	Surface Roughness	Grinding Lay Orientation	Load	Frequency	Stroke Length	Duration	Temp	Lubricant
GLO	AISI 52100 Steel	0.176 μm (45°, parallel, perpendicular) 0.028 μm (isotropic)	45°, parallel, perpendicular, isotropic	1.96 N	50 Hz	1 mm	75 min	60 °C	F-24
TS	AISI 52100 Steel	0.176 μm	Perpendicular	1.96 N	50 Hz	1 mm	75 min	60 °C, 40 °C, 30 °C	F-24
CBM	AISI 52100 Steel, Al_2O_3, Si_3N_4	0.028 μm	Isotropic	1.96 N	50 Hz	1 mm	75 min	60 °C	F-24
LP1	Al_2O_3	0.176 μm (AISI 52100 Steel) 3.413 μm (PTI 76) 4.776 μm (PTI 188) 3.602 μm (PTI 226)	Perpendicular (AISI 52100 Steel) Isotropic (PTI 76, PTI 188, PTI 226)	0.11–4.0 N	25 Hz	5 mm	60 min	40 °C	F-24
LP2	Al_2O_3	0.176 μm (AISI 52100 Steel) 3.413 μm (PTI 76) 4.776 μm (PTI 188) 3.602 μm (PTI 226)	Perpendicular (AISI 52100 Steel) Isotropic (PTI 76, PTI 188, PTI 226)	1.0 N (210 s) + 1.0–18.0 N (30 min)	25 Hz	5 mm	33.5 min	40 °C	F-24, Ethanol

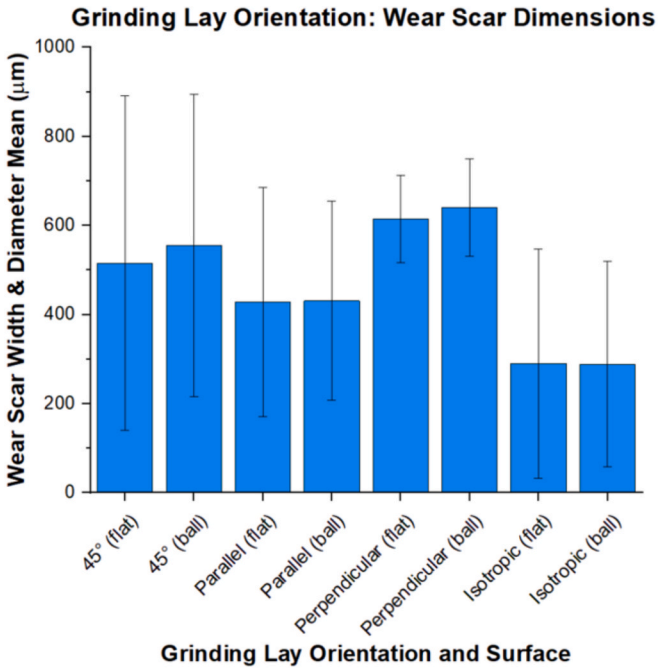

Fig. 1. Wear Scar Dimensions for GLO Investigation. Experiments were conducted using AISI 52100 steel counter bodies and plates (R_a = 0.176 ± 0.003 μm), a normal load of 1.96 N, the frequency of 50 Hz, the stroke length of 1 mm, the temperature of 60 °C, F-24 aviation fuel as a lubricant, and a duration of 75 min.

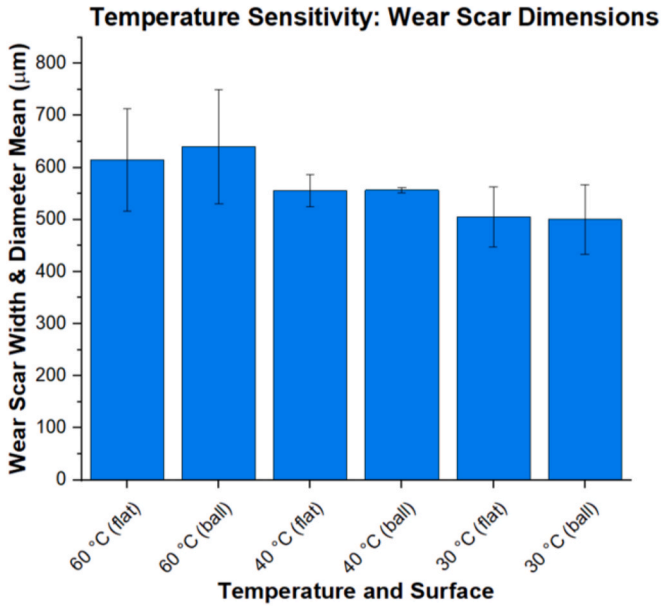

Fig. 2. Wear Scar Dimensions for TS Investigation. Experiments were conducted using AISI 52100 steel counter bodies and plates (R_a = 0.176 ± 0.003 μm), a perpendicular grinding lay orientation, a normal load of 1.96 N, frequency of 50 Hz, the stroke length of 1 mm, F-24 aviation fuel as a lubricant, and a duration of 75 min.

[12–16]. Their major requirement was to reach the scuffing regime over a short duration of the tests and modified conditions, such as the sliding velocity, displacement, fluid temperature, interface type, and load, and relate those results for the parameters for the applications where the scuffing was predicted. The design of such tests not only allows evaluation of the application parameters but also rapid assessments of suggested improvements in the materials and protective coatings.

The components of fuel system assemblies that experience scuffing are commonly made of alloy steels, such as AISI 52100 steel. Understanding the failure of steel components in sliding contacts is, therefore, important for identifying potential solutions to the issue of scuffing in fuel systems. AISI 52100 steel components typically present low frictional values when operating under lubricated conditions and show a relatively low tendency of failure [17–19]. Such behavior in steel has been explained by the presence of iron carbide (cementite) formed within the steel matrix [20,21]. The cementite particles create an extremely hard and brittle substructure capable of withstanding friction and wear caused by steel on steel interactions. The drawback, however, is the fact that variations in the operating conditions may lead to failure of the fuel lubricity and result in the high friction between sliding steel surfaces.

Here we use a high-frequency reciprocating tribometer to determine a set of tribological experimental parameters that instigate material scuffing and yield reliable and repeatable results. The ASTM D6079 standard [22] utilizing the High-Frequency Reciprocating Rig was used as a basis for the development of new experimental parameters.

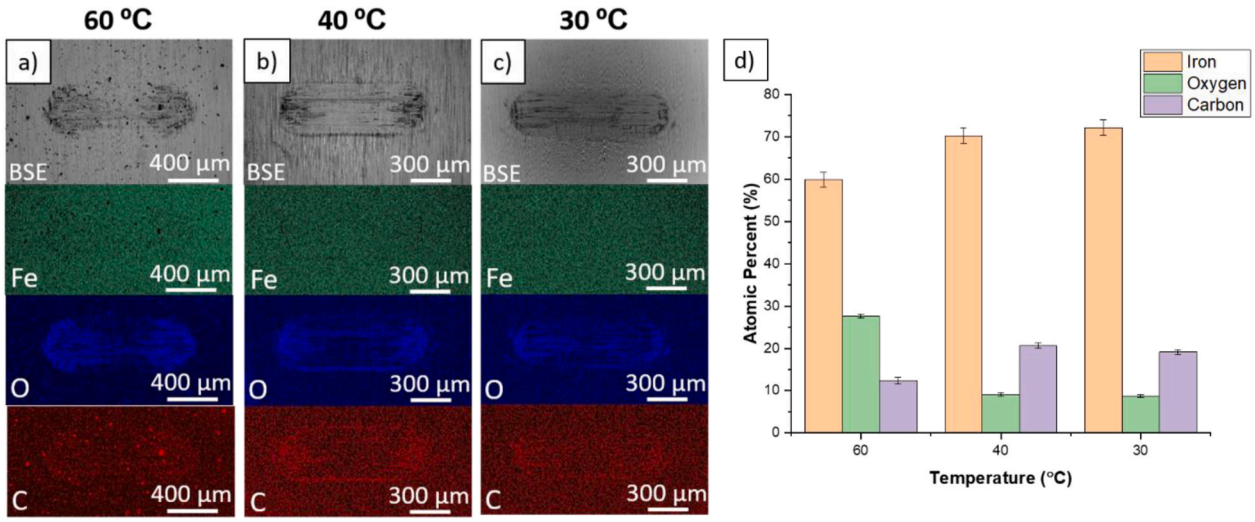

Fig. 3. SEM backscattered electron images, iron EDS maps, oxygen EDS maps, and carbon EDS maps (from top to bottom) for experiments conducted at a) 60 °C, b) 40 °C, and c) 30 °C, and d) atomic percentages of iron, oxygen, and carbon within wear scars averaged over the area inside the wear track. Experiments were conducted using AISI 52100 steel counter bodies and plates ($R_a = 0.176 \pm 0.003$ µm), a perpendicular grinding lay orientation, a normal load of 1.96 N, frequency of 50 Hz, the stroke length of 1 mm, F-24 aviation fuel as a lubricant, and a duration of 75 min.

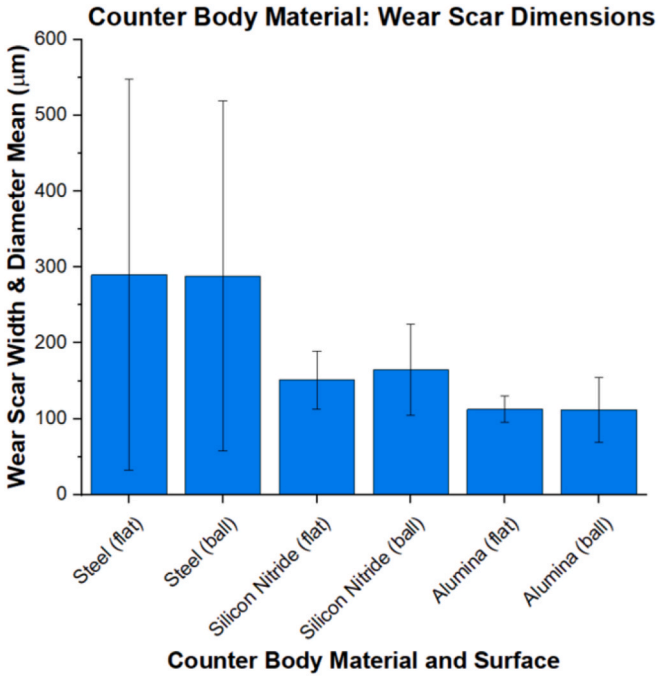

Fig. 4. Wear Scar Dimensions for CBM Investigation. Experiments were conducted using AISI 52100 steel plates ($R_a = 0.028 \pm 0.003$ µm) with isotropic grinding lay orientation, a normal load of 1.96 N, frequency of 50 Hz, the stroke length of 1 mm, the temperature of 60 °C, F-24 aviation fuel as a lubricant, and a duration of 75 min.

Reciprocating contact is found in many fuel-lubricated interfaces in machinery like fuel pumps, as are localized areas of high contact stress even in otherwise conformal contacts. This standard is commonly used to determine fuel lubricity of heavy fuels, however we sought to evaluate the variations in contact material behavior with fuels. Therefore, the experimental parameters, such as grinding lay orientation, temperature, counter body material, substrate, contact load, and stroke length were altered to determine the onset of scuffing in through-hardened 52100 steel substrates and hard coatings. Our results suggest a detailed experimental approach for evaluating lubrication failure of several materials in F-24 and ethanol, and for assessing the tribological performance of protective coatings, as demonstrated with a cobalt-based alloy and tungsten carbide coatings.

2. Experimental procedure

2.1. Materials and fuels

The experimental materials used in this study include AISI 52100 steel, silicon nitride (Si_3N_4), alumina (Al_2O_3), thermal spray coatings of PTI 76 (Co-Cr-Mo alloy), PTI 188 (WC-17Co), and PTI 226 (WC-10Co-4Cr). The lubricants used were ethanol and F-24 jet aviation fuel. AISI 52100 steel was chosen as a tribological flat specimen to represent the steels traditionally used in heavy fuel (diesel) engine fuel system components. The AISI 52100 steel specimens were through-hardened to a hardness value of 782 $HV_{0.5}$ (~62 HRC). The Co-Cr-Mo alloy, WC-17Co, and WC-10Co-4Cr were chosen as coating candidates because of their promising wear resistance characteristics reported previously in literature [23–25]. The hardness of the AISI 52100 steel and the coatings were measured with a Wilson VH1102 (Buehler) Vickers hardness tester. The microhardness values of the Co- Cr-Mo alloy, WC-17Co, and WC-10Co-4Cr were 649 ± 32 $HV_{0.5}$, 1067 ± 108 $HV_{0.5}$, and 1076 ± 97 $HV_{0.5}$, respectively. All three coatings were plasma thermally sprayed on the steel surfaces using the previously reported procedures of High Velocity Oxygen Fuel (HVOF) process using Stellite Jet Kote gun [26]. The process used hydrogen & oxygen as fuel and the coatings were produced with powders of the alloys as feed stock. The particle velocity was over in the range of 400–500 m/s and their temperature ranged from 1900 up to 2200 °C. This projectile dynamics during HVOF process ensured excellent adhesion and dense coatings leading to their very high wear resistance. The adhesion of the coatings to the substrate were measured according to the ASTM standard C633 bond pull test and exceeded 10, 000 psi for all three coating materials. The porosity of the coatings were measured by the photo standard and was found to be less than 1% for all three coatings.

Two different surface finishes were used to investigate the effect of grinding lay orientation. For the perpendicular, parallel, and 45° grinding lay orientations, the surface roughness of the steel specimens was due to the final linear grinding procedure during specimen finishing, with an average surface roughness (R_a) of 0.176 ± 0.003 µm. For the isotropic grinding lay orientation, the steel specimens were polished by

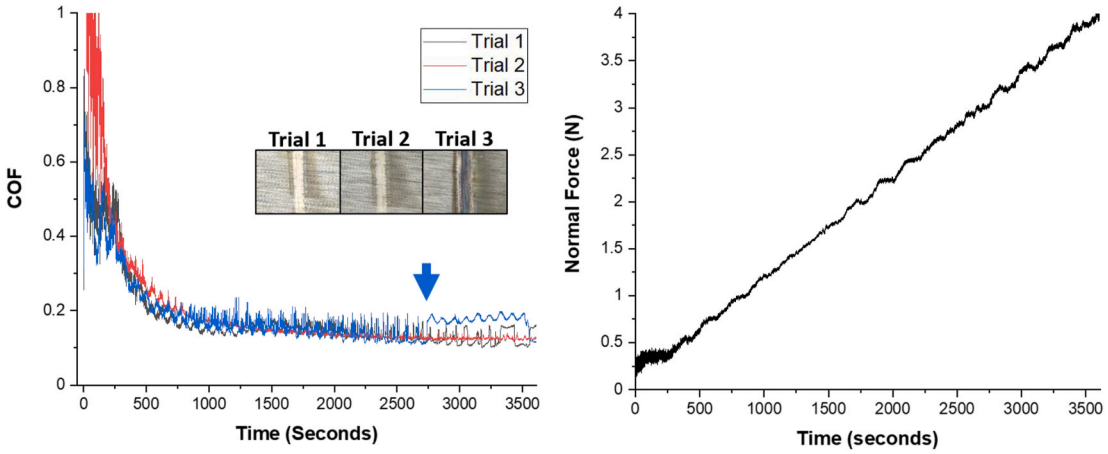

Fig. 5. COF vs. Time results for LP1 experiments in F-24 (left) and corresponding normal force vs. time plot (right). Insets are the optical images of the wear scars formed on flat steel surfaces. Experiments were conducted using AISI 52100 steel plates ($R_a = 0.176 \pm 0.003$ μm), Al_2O_3 counter bodies, perpendicular grinding lay orientation, a normal load progression of 0.11 – 4.0 N, frequency of 25 Hz, the stroke length of 5 mm, the temperature of 40 °C, F-24 aviation fuel as a lubricant, and a duration of 60 min.

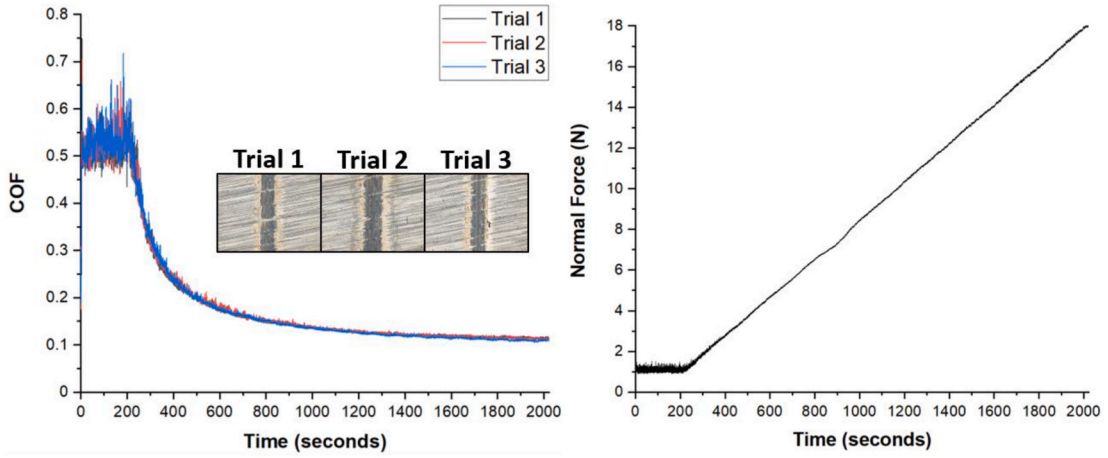

Fig. 6. COF vs. Time results for LP2 experiments in F-24 (left) and corresponding normal force vs. time plot (right). Insets are the optical images of the wear scars formed on flat steel surfaces. Experiments were conducted using AISI 52100 steel plates ($R_a = 0.176 \pm 0.003$ μm), Al_2O_3 counter bodies, perpendicular grinding lay orientation, a normal load progression of 1.0 – 18.0 N, frequency of 25 Hz, the stroke length of 5 mm, the temperature of 40 °C, F-24 aviation fuel as a lubricant, and a duration of 34 min.

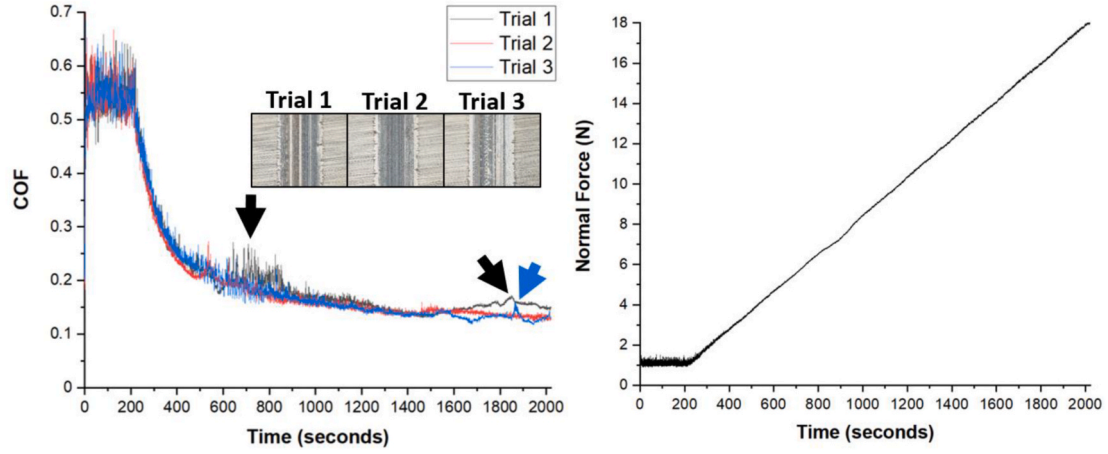

Fig. 7. COF vs. Time results for LP2 experiments in ethanol (left) and corresponding normal force vs. time plot (right). Insets are the optical images of the wear scars formed on flat steel surfaces. Experiments were conducted using AISI 52100 steel plates ($R_a = 0.176 \pm 0.003$ μm), Al_2O_3 counter bodies, perpendicular grinding lay orientation, a normal load progression of 1.0 – 18.0 N, frequency of 25 Hz, the stroke length of 5 mm, the temperature of 40 °C, ethanol as a lubricant, and a duration of 34 min.

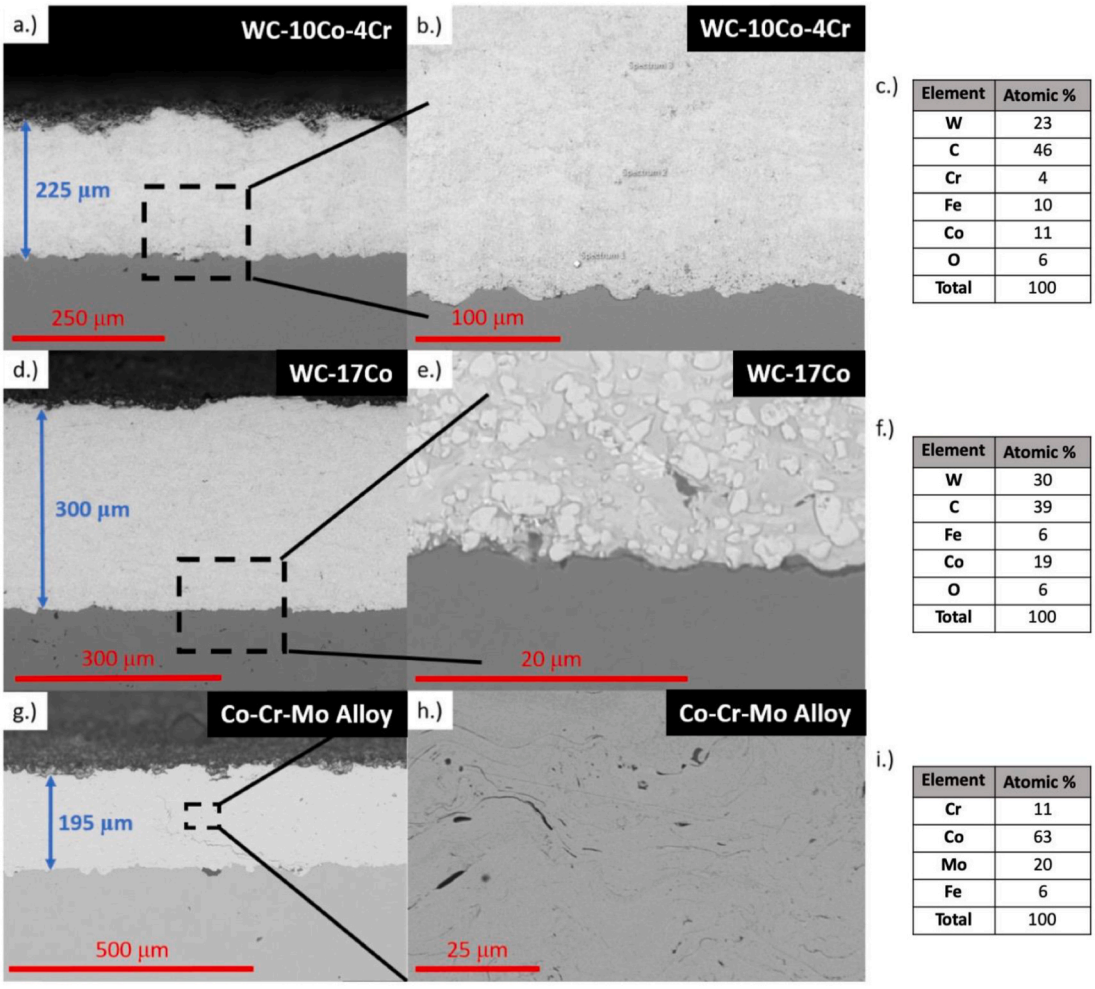

Element	Atomic %
W	23
C	46
Cr	4
Fe	10
Co	11
O	6
Total	100

Element	Atomic %
W	30
C	39
Fe	6
Co	19
O	6
Total	100

Element	Atomic %
Cr	11
Co	63
Mo	20
Fe	6
Total	100

Fig. 8. SEM images of a.) WC-10Co-4Cr coating cross-section, b.) WC-10Co-4Cr coating/substrate interface, and c.) WC-10Co-4Cr composition. SEM images of d.) WC-17Co coating cross-section, e.) WC-17Co coating/substrate interface, and f.) WC-17Co composition. SEM images of g.) Co-Cr-Mo alloy coating cross-section, h.) Co-Cr-Mo alloy coating, and i.) Co-Cr-Mo alloy composition.

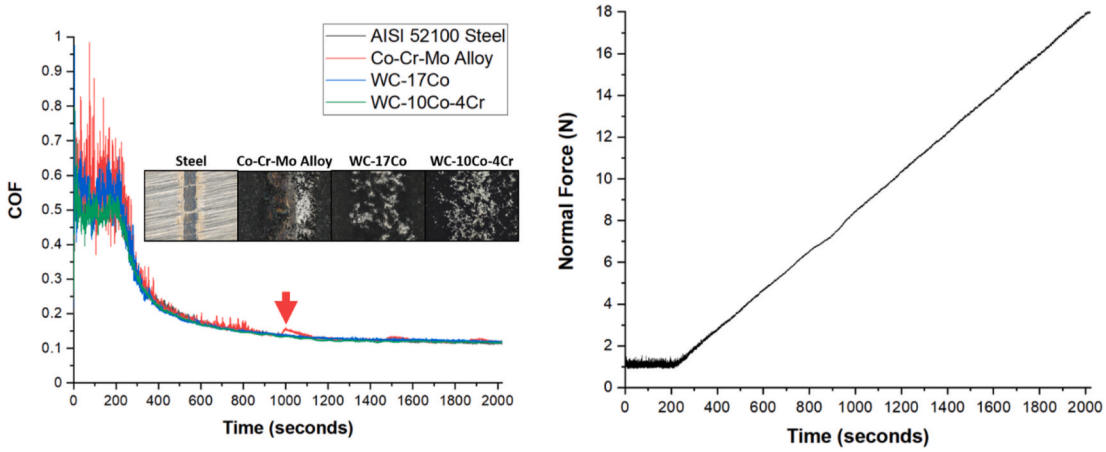

Fig. 9. COF vs. Time results for LP2 experiments on AISI 52100 steel and various coatings in F-24 jet aviation fuel (left) and corresponding normal force vs. time plot (right). Insets are the optical images of the wear scars formed on flat surfaces. Experiments were conducted using several plate materials (AISI 52100 steel, Co-Cr-Mo alloy, WC-17Co, and WC-10Co-4Cr), Al_2O_3 counter bodies, a normal load progression of 1.0 – 18.0 N, frequency of 25 Hz, the stroke length of 5 mm, the temperature of 40 °C, F-24 aviation fuel as a lubricant, and a duration of 34 min.

hand to an average surface roughness of 0.028 ± 0.003 µm. The R_a for the steel specimens was measured with a Zygo ZeGage Plus Optical Profilometer.

Three different counter body materials were used to investigate the effect of counter body material: hardened AISI 52100 steel, Si_3N_4, and Al_2O_3. All three counter body balls had a diameter of 6 mm. The

Table 2
Time of first COF increase and wear scar width of flat specimen for LP2 experiments performed on AISI 52100 steel and coatings in F-24 and ethanol.

Flat Material	Lubricant	Trial #	Time of First COF Increase	Flat Wear Scar Width
AISI 52100 Steel	F-24	1	–	186.6 μm
		2	–	218.4 μm
		3	–	226.0 μm
	Ethanol	1	626 s	340.5 μm
		2	537 s	333.7 μm
		3	1867 s	354.9 μm
Co-Cr-Mo alloy (PTI 76)	F-24	1	–	593.1 μm
		2	680 s	873.7 μm
		3	996 s	884.3 μm
	Ethanol	1	–	875.2 μm
		2	–	711.4 μm
		3	–	1014.7 μm
WC-17Co (PTI 188)	F-24	1	–	993.5 μm
		2	–	973.8 μm
		3	–	1011.7 μm
	Ethanol	1	–	1214.9 μm
		2	1386 s	1218.0 μm
		3	–	1072.4 μm
WC-10Co-4Cr (PTI 226)	F-24	1	–	1601.7 μm
		2	–	1148.2 μm
		3	–	1022.3 μm
	Ethanol	1	–	1034.4. μm
		2	–	970.7 μm
		3	–	1067.8 μm

grinding lay orientation investigation, temperature sensitivity investigation, and counter body material investigation experiments were conducted with F-24 jet aviation fuel as lubricant. The load progression investigation experiments were conducted with both F-24 jet aviation fuel and ethanol. F-24 and Ethanol have a viscosity at 40 °C of approximately 1.36 cSt and 1.08 cSt [27], respectively, a viscosity substantially lower than for most lubricants and diesel fuel.

2.2. Measurement method overview

The tribometer used in this study is a CETR UMT-3 pin-on-plate tribometer. This tribological contact geometry was chosen due to its allowance of precise control of the contact conditions between the reciprocating flat and static counter body ball. The diameters of the ball counter bodies used were 6 mm with at least a 3 mm spacing interval between experiments on the flat surface.

The output data used from the tribometer is the coefficient of friction (COF) between the counter body and plate throughout experiments. The COF is obtained from the applied load and the measured lateral forces of friction between the counter body and plate, as measured by strain-gauge load cells. A sample was considered to have scuffed if the COF data for an experiment exhibited a sudden and sustained increase in the COF during the experiment.

The tribometer was used to conduct high-velocity experiments with static loads as well as load progressions, as outlined in Table 1. Notably, the sliding velocities tested in the proposed experiments are fairly low in comparison to the velocities observed in the heavy fuel engine fuel system applications. This low velocity in comparison to component speeds in fuel systems is not expected to be an issue, because scuffing was previously observed at the ends of the wear track where the velocities reduce to zero at the turn-around points and result in a thinning and potential breakdown of the protective lubricant film [12]. Another condition difficult to mimic is the fluid temperature, as the temperature may vary drastically depending on the environment in which the mechanical system is operated. Here we chose the range of temperatures to test the reproducibility of the scuffing events.

The ASTM D6079 standard for evaluating the lubricity of diesel fuels by the high-frequency reciprocating rig [22] was chosen as the basis for the experimental method developed in this study due to its inclusion of high-frequency reciprocating tribological contacts [28]. Of the existing parameters in the ASTM D6079 standard [22], the counter body material, grinding lay orientation, load, frequency, stroke length, experimental duration, temperature, and lubrication were changed to conduct the following investigations:

- Grinding Lay Orientation Investigation (denoted at GLO): the orientation of the counter body movement relative to the grinding lay of the flat steel specimens was investigated in four values - 45°, parallel, perpendicular, and isotropic as to determine which orientation provided the most repeatable results.
- Temperature Sensitivity Investigation (denoted as TS): the temperature of experiments was investigated in three values - 60 °C, 40 °C, 30 °C as to determine if lowering the temperature would drastically affect the results of experiments, preserve fuel in the tribometer reservoir due to evaporation, and make results more repeatable.
- Counter Body Material Investigation (denoted as CBM): the counter body material was investigated for three different materials – AISI 52100 steel, Al_2O_3, and Si_3N_4 as to determine which material provided the most repeatable results and which wore the least to be capable of imparting damage on hard ceramic coatings.
- Load Progression Investigation, 0.11 N – 4.0 N (denoted as LP1): the load used during experiments was changed from static to a linear progression as to attempt to instigate scuffing. This load range was chosen based on the limitations of the 5 N load cell utilized for these experiments. In addition, the frequency of 25 Hz and stroke length of 5 mm were implemented to increase the maximum linear sliding velocity to 0.25 m/s. This sliding velocity was increased to better represent the sliding velocities typically used in fuel injection systems while falling within the UMT-3 operating envelope.
- Load Progression Investigation, 1.0 – 18.0 N (denoted as LP2): the load used during experiments was changed to an initial static load of 1.0 N for a 210 s run-in period, followed by a linear progression. The load range used to investigate the effect on the instigation of scuffing events was limited by the load cell parameters.

After experiments were completed, the counter bodies and flat specimens were removed and rinsed with acetone, followed by hexane, and then isopropyl alcohol. The wear tracks were imaged using a Zeiss LSM 700 Optical Microscope. The samples were also characterized using a Hitachi SV3500 Scanning Electron Microscope (SEM) equipped with Electron Dispersive Spectroscopy (EDS) to assess any changes in elemental concentration on the specimen surfaces during experiments. From the calibrated optical microscope images, the wear scar diameter of the worn counter bodies was calculated per the ASTM D6079 standard [22], as follows:

$$WSD = \frac{M+N}{2}$$

Where WSD is the wear scar diameter in μm, M is the diameter in the x-axis (perpendicular to sliding) in μm, and N is the diameter in the y-axis (parallel to sliding) in μm [22]. Wear scar dimension on the flat surface was recorded perpendicular to the sliding direction in the center of the wear track.

3. Results and discussion

3.1. Grinding lay orientation investigation

The wear scar dimensions for both the flat steel specimens and AISI 52100 steel counter bodies for the experiments concerning the GLO investigation are presented in Fig. 1. Three experiments were conducted for each of the grinding lay orientations. The error bars shown in Fig. 1 were calculated using a 90% confidence interval with two-sided t-distribution. Based on the error values, the perpendicular grinding lay

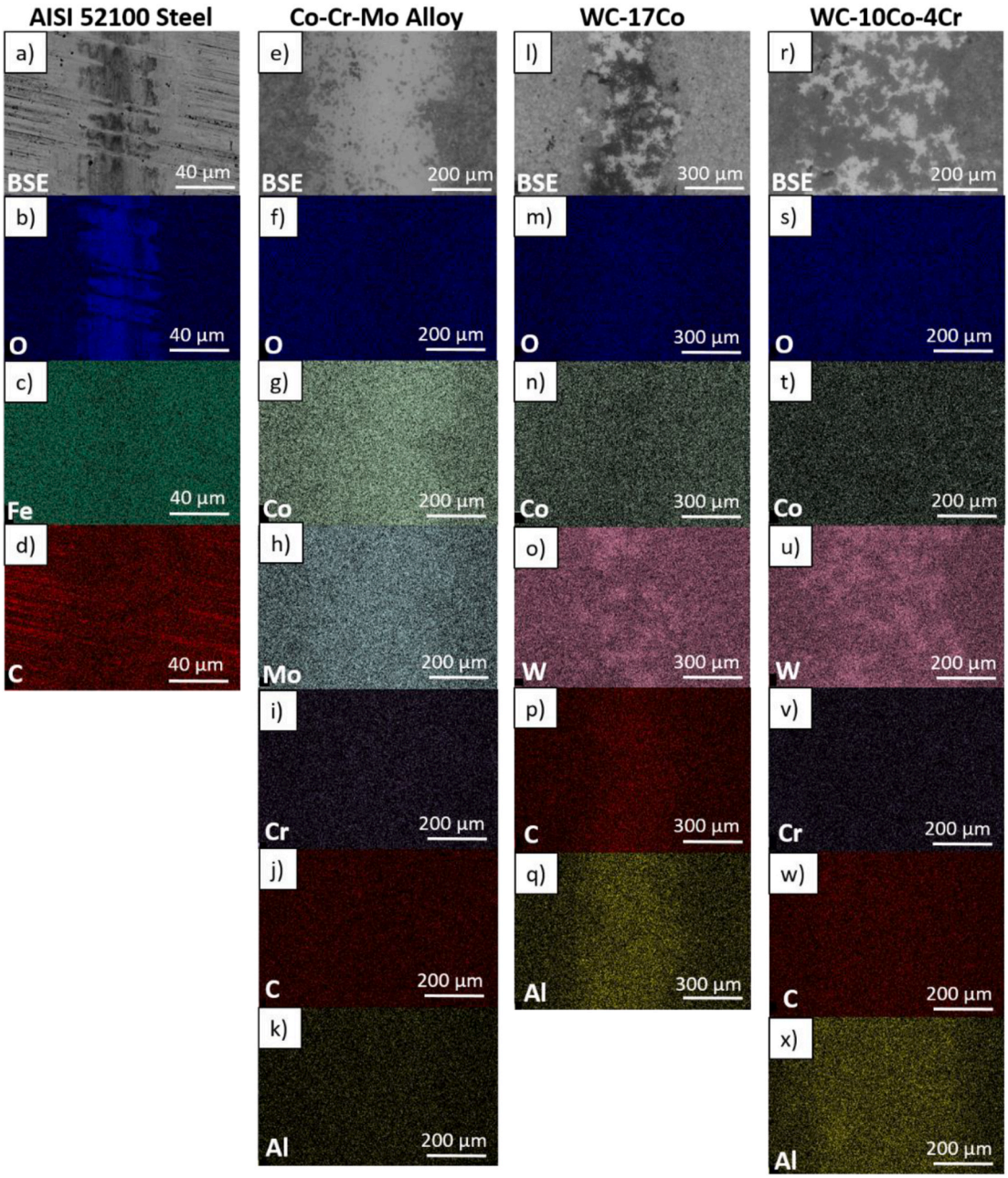

Fig. 10. EDX images of wear scars created during experiments using the LP2 parameter set and F-24 jet aviation fuel. AISI 52100 steel flat substrate: a) SEM image, b) oxygen, c) iron, d) carbon. Co-Cr-Mo alloy flat substrate: e) SEM image, f) oxygen, g) cobalt, h) molybdenum, i) chromium, j) carbon, k) aluminum. WC-17Co flat substrate: l) SEM image, m) oxygen, n) cobalt, o) tungsten, p) carbon, q) aluminum. WC-10Co-4Cr flat substrate:r) SEM image, s) oxygen, t) cobalt, u) tungsten, v) chromium, w) carbon, x) aluminum. Experiments were conducted using several plate materials (AISI 52100 steel, Co-Cr-Mo alloy, WC-17Co, and WC-10Co-4Cr), Al_2O_3 counter bodies, a normal load progression of 1.0 – 18.0 N, frequency of 25 Hz, the stroke length of 5 mm, the temperature of 40 °C, F-24 aviation fuel as a lubricant, and a duration of 34 min.

orientation provided the most repeatable results. Therefore, it was selected for the following experiments.

3.2. Temperature sensitivity investigation

The temperature fluctuations in the engine components may differ significantly but are estimated to fall within the range of −20 °C to over 100 °C [29]. As a precise operating temperature is not established, this study aimed to reduce the experimental temperature of the ASTM D6079 standard [26] to preserve the fuels used during experiments, increase the repeatability of results, and aid data analysis for the experiments.

The wear scar dimensions for both the flat steel specimens and AISI 52100 steel counter bodies for the experiments concerning the temperature sensitivity investigation are presented in Fig. 2. The experiments at each temperature were repeated 2 to 3 times to determine the consistency of the results. The error bars shown in Fig. 2 were calculated using a 90% confidence interval with two-sided t-distribution. The error values indicate that when the temperature was lowered from 60 °C to 40 °C the repeatability of results was improved. In addition to error calculations, ANOVA analysis was used to calculate the p-value for the wear scar dimensions for experiments performed at the three temperatures. The p-value for the wear scar widths on flat specimens is 0.07, which is greater than the critical p-value 0.05, indicating that the difference between the flat wear scar width values at the varying

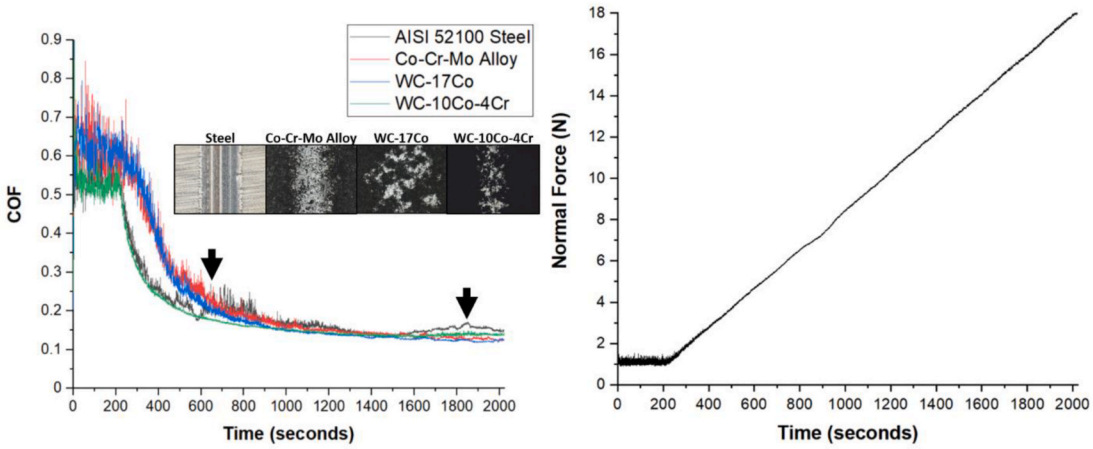

Fig. 11. COF vs. Time results for LP2 experiments on AISI 52100 steel and various coatings in ethanol (left) and corresponding normal force vs. time plot (right). Insets are the optical images of the wear scars formed on flat surfaces. Experiments were conducted using several plate materials (AISI 52100 steel, Co-Cr-Mo alloy, WC-17Co, and WC-10Co-4Cr), Al_2O_3 counter bodies, a normal load progression of 1.0 – 18.0 N, frequency of 25 Hz, stroke length of 5 mm, temperature of 40 °C, ethanol as lubricant, and a duration of 34 min.

temperatures is not statistically significant.

EDS mapping of the wear scars formed on the steel plates during the TS investigation experiments are shown in Fig. 3. The EDS maps for experiments conducted indicates that lowering the temperature of experiments did not significantly alter the distribution of oxygen within the wear scars. Fig. 3.d shows the atomic percentages of iron, oxygen, and carbon within the wear scars, as determined by selecting the wear scar area with EDS. As shown in Fig. 3.d, the amounts of oxygen within the wear scars for experiments conducted at 30 °C and 40 °C were similar, but in the experiment conducted at 60 °C the oxygen amount nearly doubled that suggests high importance of the temperature conditions on the resulting performance of the materials. In addition, the viscosity of fuels and lubricants tends to be reported at 40 °C, thus introducing this temperature to the experimental method aids the analysis of results in future studies where the method is extended to different fuels. The enhanced repeatability of results and availability of fuel viscosity data resulted in the establishment of 40 °C as the temperature used in further experiments.

3.3. Counter body material investigation

While the first experiments conducted in this study aimed to produce scuffing on AISI 52100 steel specimens, the experimental method was also extended to other materials, including hard ceramic coatings. Thus, altering the counter body material established in the ASTM D6079 standard [22] was investigated to determine an accessible ceramic material that resists wear against other hard materials and improves the repeatability of results. This investigation was used to determine a material that will impart tribological damage to hard protective coatings, thus allowing for evaluation of the materials resistance to scuffing.

The wear scar dimensions for both the flat steel specimens and the AISI 52100 steel, Al_2O_3, and Si_3N_4 counter bodies for the experiments concerning the CBM investigation are presented in Fig. 4. Three experiments were conducted for each of the counter body materials. The error bars shown in Fig. 4 were calculated using a 90% confidence interval with two-sided t-distribution. Based on the error values, the Al_2O_3 counter bodies provided the most repeatable results. The Al_2O_3 counter body exhibited the smallest amount of wear compared to the AISI 52100 steel and Si_3N_4 counter bodies, indicating Al_2O_3 is the best material choice in developing an experimental method that can impart tribological damage to AISI 52100 steel flats as well as hard ceramic protective coatings.

3.4. Load progression investigation on AISI 52100 steel

Load progressions, as opposed to static loads, have shown to aid in the instigation of the scuffing, such as in the studies of Suh et al. [14] and Riggs et al. [16]. The COF vs. time plots for the experiments conducted for the GLO, TS, and CBM investigations which utilized static loads (1.96 N) did not show a sudden and sustained increase in COF that is used here as one of the indications of scuffing. The first load progression chosen in this study was 0.11–4.0 N (LP1), with a linear increase in load over the span of the 60 min experiment. This small and low range of contact load, as well as 60 min experiment duration, were chosen to reflect the low loads that certain mechanical systems, such as engine fuel system components, experience during operation [30].

For the LP1 parameter set experiments using F-24 aviation fuel, the resulting COF vs. time data and optical images are shown in Fig. 5. Of the three experiments conducted, the third experiment (denoted as "Trial 3" in Fig. 5) exhibited a sudden increase in COF at approximately 2750 s, correlating to a load of approximately 3 N. Also, the optical image of the flat steel wear scar corresponding to "Trial 3" is darker in comparison to the other two experiments, indicating this wear track experienced more oxidation [16]. Both the sudden increase in the COF and the greater extent of corrosion present for "Trial 3" indicate that scuffing occurred.

After scuffing was successfully initiated using the LP1 parameter set, a run-in period with a 1.0 N load and 210 s duration was introduced to an increased load progression range (1.0–18.0 N). The load progression duration was decreased to 30 min for the parameter set LP2 (Fig. 6). These parameter changes were made to investigate whether making the load progression more aggressive would increase the likelihood to instigate scuffing. For the LP2 parameter set experiments using F-24 aviation fuel, the resulting COF vs. time data and optical images are shown in Fig. 6. As seen in the COF vs. time data, none of the three experiments exhibited a sudden increase in the COF. Besides, all three of the flat steel wear scars show similar levels of corrosion visually due to the more aggressive loading. Thus, it is concluded that no scuffing occurred under the higher load progression in the presence of F-24 aviation fuel.

To assess the effect of lubrication with a less lubricious fuel using method LP2, three additional experiments were performed with ethanol instead of F-24 aviation fuel. Ethanol has a low viscosity [27] with no lubrication-aiding additives (unlike F-24). For the LP2 parameter set experiments using ethanol, the resulting COF vs. time data and optical images are shown in Fig. 7. The first experiment conducted (denoted as "Trial 1" in Fig. 7) exhibited an increase in COF at approximately 400 s,

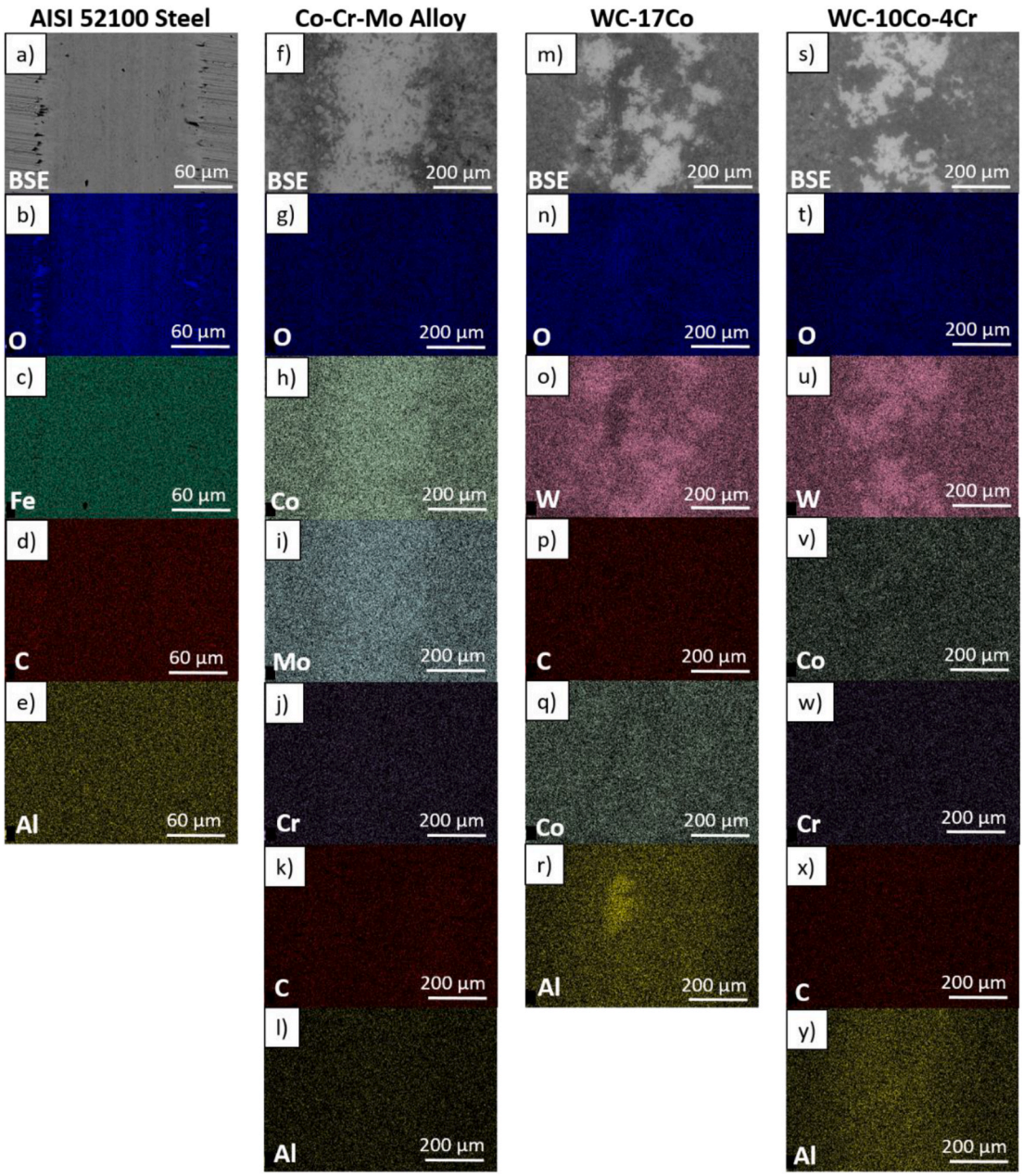

Fig. 12. EDX images of wear scars created during experiments using the LP2 parameter set and ethanol. AISI 52100 steel flat substrate: a) SEM image, b) oxygen, c) iron, d) carbon, e) aluminum. Co-Cr-Mo alloy flat substrate: f) SEM image, g) oxygen, h) cobalt, i) molybdenum, j) chromium, k) carbon, l) aluminum. WC-17Co flat substrate: m) SEM image, n) oxygen, o) tungsten, p) carbon, q) cobalt, r) aluminum. WC-10Co-4Cr flat substrate: s) SEM image, t) oxygen, u) tungsten, v) cobalt, w) chromium, x) carbon, y) aluminum. Experiments were conducted using several plate materials (AISI 52100 steel, Co-Cr-Mo alloy, WC-17Co, and WC-10Co-4Cr), Al_2O_3 counter bodies, a normal load progression of 1.0 – 18.0 N, frequency of 25 Hz, the stroke length of 5 mm, the temperature of 40 °C, ethanol as a lubricant, and a duration of 34 min.

correlating with a load of approximately 15 N, followed by a second increase in COF at approximately 1650 s. These two increases in COF correlate with approximate loads of 5 N and 15 N, respectively. The third experiment (denoted as "Trial 3" in Fig. 7) shows an increase in COF at approximately 1650 s, correlating with a load of 15 N. However, in contrast to the results of "Trial 3" in LP1, this increase in COF did not occur suddenly, but was achieved over about 200-s period. The optical images of the flat steel wear scars for all three experiments using LP2 in ethanol show corrosion, however with varying distributions. The peak in COF for "Trial 1" and "Trial 3" and the presence of corrosion indicates that a more severe wear regime was reached, however since it occurred over an extended amount of time it cannot be precisely stated to indicate a scuffing event occurred [12,31].

3.5. Load progression investigation on protective coatings

To assess the effectiveness of the protective coatings in inhibiting the initiation of scuffing, LP2 parameter set experiments were performed on three protective coatings (Co-Cr-Mo alloy, WC-17Co, and WC-10Co-4Cr). SEM images and the composition of these coatings (determined with EDS) analysis are shown in Fig. 8. These coatings have a thickness ranging from approximately 200 µm–300 µm and were chosen for analysis due to their wear resistance [23–25].

Three to five trials were conducted for each coating in each fuel. For the LP2 parameter set experiments that used F-24 aviation fuel, the resulting COF vs. time data and the corresponding optical images of the formed wear tracks are shown in Fig. 9 for a representative trial. It was

observed that the COF values during the load progression for Co-Cr-Mo alloy included sharp increases in two trials (see Table 2), whereas both WC-based coatings did not have any increases in COF and fell steadily. For Co-Cr-Mo alloy, the earliest increase in the COF occurred at approximately 470 s in one trial and 786 s in the other trial, corresponding to approximate loads of 5 N and 8 N, respectively. The optical images in Fig. 9 show a darker track on the steel specimen and lighter patches in the wear tracks of the two WC-based coatings and the Cr-Co-Mo alloy coating. The lighter patches in these coatings corresponded to flatter areas that reflect more light, indicating a polishing of the topmost asperities of these comparatively (to steel) rough coatings. The optical images in Fig. 9 and wear scar width values in Table 2 show that the wear scars on the WC-based coatings are significantly wider than those produced on the AISI 52100 steel specimens. While the WC-based coating wear tracks have greater width values than that of the steel specimens, it is also noted that the wear marks on these specimens are in the form of patches (see Fig. 9), unlike the linear wear markings shown on the AISI 52100 steel specimens. The appearance of wear marks in isolated patches on the WC-based coatings indicates that only asperity wear occurred, and thus these materials experienced less wear relative to the less rough steel surfaces.

EDS analysis of the wear scars produced on the flat specimens during these experiments is shown in Fig. 10. The wear track of the Co-Cr-Mo alloy specimen (shown in Fig. 10.e – 10.k) did not show signs of oxidation corrosion occurring during the experiment. Thus, if the increase in the COF values of the Co-Cr-Mo alloy specimen during the experiment is indicative of scuffing, then the scuffing must have been non-oxidative. In case of the WC-17Co and WC-10Co-4Cr, the presence of aluminum in the wear track as indicated by the contrast on the 2D maps of the EDS analysis (Fig. 10.q and Fig. 10.x) suggest some material transferred from the Al_2O_3 ball, indicating that these materials were more wear-resistant as compared to AISI 52100 steel and Co-Cr-Mo alloy. Further, the increased presence of tungsten in the wear track of the WC-based coatings can be seen in patches corresponding to the brighter areas of the optical microscopy (Fig. 9). As the energy for the tungsten Mα spectral line in EDS analysis is approximately 1.8 keV [32] and tungsten has a high atomic number, these patches of high W concentration (Fig. 10.o and Fig. 10.u) are not likely to be the result of shadowing by other elements' energies [32]. Thus, the greater concentration of W present in the wear tracks for the WC-based coatings suggests that tungsten may preferentially segregate in areas of wear.

The LP2 load progression procedure was also performed on the coatings submerged in ethanol. These experiments were performed to investigate which coatings were more effective in inhibiting scuffing in the presence of a liquid of slightly lower viscosity than the F-24 jet fuel, but with drastically different chemistry. The resulting COF vs. time data and optical images of the wear tracks are shown in Fig. 11. All three trials performed on AISI 52100 steel included sharp increases in COF values, as shown in Table 2. For the AISI 52100 steel, the first increases in COF for the three trials occurred at approximately 416, 327, and 1657 s. In addition, one trial for the WC-17Co coating included an increase in COF value occurring at 1176 s, however, no increase was observed in the other two trials. For the WC-based coatings, it is possible that the conditions of the performed LP2 experiments could eventually lead to scuffing if the duration of the experiments was increased, and this increase in COF for one WC-17Co trial is indicative of this. From the data presented with the 34-min duration, however, it is evident that the WC-17Co coating is more resistant to scuffing than AISI 52100 steel. Specifically, the COF does not show any sudden increase in the value and optical images of the wear track suggest uniform flattening of the asperities similarly to the test in F-24. The WC-10Co-4Cr and Co-Cr-Mo alloy coatings did not show any increase in COF indicative of scuffing during any trials.

EDS analysis of the wear tracks produced on the flat specimens during the LP2 investigation experiments in ethanol is presented in Fig. 12. As seen in Fig. 12.b, the AISI 52100 steel wear track showed that oxidation occurred during the experiment, as seen in the linear patches of oxygen concentration. The appearance of the oxidation in linear sections, separated by areas with less oxygen, indicates that oxide layers on the AISI 52100 steel surface were formed and subsequently broken and churned during the experiment, an indication that scuffing initiated in conjunction with the increase in COF (Fig. 11). Similarly to the experiments performed in F-24 jet aviation fuel, the wear tracks have rough patchy appearance suggesting formation of broken and churned oxide layer during the experiments in ethanol performed using the Co-Cr-Mo alloy flat specimen (Fig. 12g). In addition, Fig. 12.r and Fig. 12.y show through the presence of aluminum in the wear track that material transfer from the Al_2O_3 counter body to the WC-17Co and WC-10Co-4Cr substrates occurred. This shows that WC-17Co and WC-10Co-4Cr are wear-resistant not only in F-24 jet aviation fuel, but also in ethanol lubrication. EDS analysis of the wear tracks for tungsten carbide specimens indicates patchy nature of W, similarly to F-24 fuel.

There are differences not only between the tribological performance of the steel and the coatings, but differences between the materials' behaviors when worn in the two different fuels used. For example, the wear track widths are greater for experiments performed with ethanol lubrication for the AISI 52100 steel, Co-Cr-Mo alloy, and WC-17Co specimens (see Table 2). This can be attributed to the higher viscosity of F-24 fuel relative to ethanol, as the higher viscosity allows for thicker protective lubricant films to form and less direct contact between the specimens and counter bodies. However, the WC-10Co-4Cr wear tracks produced in ethanol have smaller widths than those produced in F-24 (see Table 2). This may be attributed to the chromium content in the WC-10Co-4Cr coating, as in the electromotive series of metals chromium has a greater potential to oxidize than cobalt [33].

Another contrast between the experiments performed in F-24 and ethanol is the visual appearance of the wear scars produced on the flat specimens. As seen in Fig. 9, some of the perpendicular machining marks are left within the wear scar produced on the AISI 52100 steel flat in F-24 lubrication. In Fig. 11, the wear scar on the steel specimen produced within ethanol does not retain any machining marks, indicating that the steel specimen experienced more wear when submerged in ethanol. For the WC-based coatings, Figs. 9 and 11 show similar bright areas indicative of asperity polishing when tested in two fuels. The Co-Cr-Mo alloy wear scar appearance differs in coloration depending on the fuel used during experiments. In Fig. 9, some discoloration of the wear track on the left-hand side is present for the wear track produced in F-24, while the wear track produced in ethanol (see Fig. 11) lacks this discoloration. This difference in the appearance of the wear scars may be attributed to the roughness variations of the wear scars and some residual contamination from the fuel during optical microscopy imaging. The Co-Cr-Mo alloy specimen submerged in ethanol experienced more asperity wear than that produced in F-24 due to the thinner lubricant film provided by ethanol. This greater extent of asperity smoothening provides a wear scar that is less rough and more reflective. The Co-Cr-Mo alloy specimen wear scar produced in F-24 experienced less smoothening of asperities due to the thicker lubricant film produced by F-24, perhaps leading to more abrasive wear and producing the discoloration of the wear scar presented in Fig. 11.

The results indicate that the Co-Cr-Mo alloy shows evidence of scuffing in F-24 fuel (see the increases in COF in Fig. 9) while there is no evidence of scuffing for the experiments performed in ethanol, which may be attributed to the chemistry of the fuels. It should be emphasized that the scuffing process largely depends on the synergy of several factors, including but not limited to abrasive wear, oxidation of the material, material hardness, surface roughness, adhesion between material grains, and viscosity of the lubricant. Presence of the layered defects in Co-Cr-Mo, as observed in the SEM images of the coating cross-sections in Fig. 8 suggests that this coating candidate might be more vulnerable to the scuffing processes.

4. Conclusions

In conclusion, we created a detailed study of scuffing initiation in sliding steel components lubricated by low-viscosity fuels such as ethanol. By varying the temperature of the experiments, grinding lay orientation, counter body material, and load we established the set of parameters leading to reproducible friction and wear of the steel surfaces. Specifically, we demonstrated that the perpendicular grinding lay orientation provides the most repeatable results. Variations in the temperature from 30 to 60 °C had almost no effect on the wear scar dimensions and repeatability of results. Variation in the counter body material suggested that use of alumina results in the most repeatable results which is attributed to the limited wear of the ball surfaces in comparison to steel.

We further tested the method for scuffing analysis with three coating candidates, Co-Cr-Mo alloy, WC-17Co, and WC-10Co-4Cr. Load progression experiments that were performed in F-24 fuel and ethanol indicated that WC-based materials (WC-17Co and WC-10Co-4Cr) are resistant to scuffing initiation in comparison to uncoated steel surfaces. In contrast, the Co-Cr-Mo alloy indicated scuffing in lower viscosity ethanol.

Our results suggest a detailed experimental approach for evaluating scuffing resistance of materials and lubrication reliability of fluids used in mechanical components. While reproducing the same operation settings in the lab environment are challenging, the proposed method creates a more rapid evaluation of the surfaces and coatings suitability for the operation in fuel environments. Thus, the screening of the potential material candidates can be performed more efficiently.

CRediT authorship contribution statement

Kelly Jacques: Investigation, Data curation, Writing. **Nikhil Murthy:** Data curation. **Satish Dixit:** Resources. **Diana Berman:** Investigation, Formal analysis, Writing. **Stephen Berkebile:** Supervision, Investigation, Conceptualization, Writing.

Declaration of competing interest

The authors declare that they have no known competing financial interests or personal relationships that could have appeared to influence the work reported in this paper.

Acknowledgments

The authors acknowledge assistance provided by Caleb Matzke and Dr. Jon-Erik Mogonye. Research was sponsored by the Army Research Laboratory and was accomplished under Cooperative Agreement Numbers W911NF-20-2-0060, W911NF-19-2-0281, and W911NF-20-2-0198. The views and conclusions contained in this document are those of the authors and should not be interpreted as representing the official policies, either expressed or implied of the Army Research Laboratory or the U.S. Government. The U.S. Government is authorized to reproduce and distribute reprints for Government purposes notwithstanding any copyright notations herein. Parts of the research were conducted under the ARL College Qualified Leaders program.

References

[1] A.Z. Szeri, Tribology: friction, lubrication, and wear Hemisphere1980.
[2] Bowman W, Stachowiak G. A review of scuffing models. Tribol Lett 1996;2:113–31.
[3] Blok H. Seizure-delay" method for determining the seizure protection of EP lubricants. SAE Trans 1939:193–220.
[4] Blok H. Thermo-tribology—fifty years on. Institution of Mechanical Engineers, International Conference on Tribology; 1987. p. 1–8.
[5] Gecim B, Winer W. Steady temperatures in a rotating cylinder—some variations in the geometry and the thermal boundary conditions. 1986.
[6] Tian X, Kennedy Jr FE. Contact surface temperature models for finite bodies in dry and boundary lubricated sliding. 1993.
[7] Kannel J, Barber S. Analysis of scuffing temperatures with considerations of wear. 1990.
[8] Archard J. The temperature of rubbing surfaces. Wear 1959;2:438–55.
[9] Dyson A. The failure of elastohydrodynamic lubrication of circumferentially ground discs. Proc Inst Mech Eng 1976;190:699–711.
[10] Lee SC, Chen H. Experimental validation of critical temperature-pressure theory of scuffing. Tribol Trans 1995;38:738–42.
[11] Jiajun L, Zhiqiang L, Yinqian C. The study of scuffing and pitting failure of cam-tappet rubbing pair. Wear 1990;140:135–47.
[12] Qu J, Truhan JJ, Blau PJ, Meyer III HM. Scuffing transition diagrams for heavy duty diesel fuel injector materials in ultra low-sulfur fuel-lubricated environment. Wear 2005;259:1031–40.
[13] Ludema KC. A review of scuffing and running-in of lubricated surfaces, with asperities and oxides in perspective. Wear 1984;100:315–31.
[14] Suh AY, Polycarpou AA, Conry TF. Detailed surface roughness characterization of engineering surfaces undergoing tribological testing leading to scuffing. Wear 2003;255:556–68.
[15] Nilsson D, Isaksson P, Prakash B. Effects of area ratio and nature of surfaces on scuffing in lubricated contacts. Proc IME J J Eng Tribol 2009;223:445–55.
[16] Riggs MR, Murthy NK, Berkebile SP. Scuffing resistance and starved lubrication behavior in helicopter gear contacts: dependence on material, surface finish, and novel lubricants. Tribol Trans 2017;60:932–41.
[17] Shirani A, Joy T, Lager I, Yilmaz JL, Wang H-L, Jeppson S, Cahoon EB, Chapman K, Stymne S, Berman D. Lubrication characteristics of wax esters from oils produced by a genetically-enhanced oilseed crop. Tribol Int 2020;146:106234.
[18] Jacques K, Joy T, Shirani A, Berman D. Effect of water incorporation on the lubrication characteristics of synthetic oils. Tribol Lett 2019;67:105.
[19] Romsdahl T, Shirani A, Minto RE, Zhang C, Cahoon EB, Chapman KD, Berman D. Nature-guided synthesis of advanced bio-lubricants. Sci Rep 2019;9:11711.
[20] Moore M. The relationship between the abrasive wear resistance, hardness and microstructure of ferritic materials. Wear 1974;28:59–68.
[21] Perez-Unzueta AJ, Beynon JH. Microstructure and wear resistance of pearlitic rail steels. Wear 1993;162:173–82.
[22] International A. Standard test method for evaluating lubricity of diesel fuels by the high-frequency reciprocating rig (HFRR). Annual book of ASTM standards. West Conshohocken, PA: ASTM International; 2018.
[23] Neville A, Kollia-Rafailidi V. A comparison of boundary wear film formation on steel and a thermal sprayed Co/Cr/Mo coating under sliding conditions. Wear 2002;252:227–39.
[24] Ozdemir I. Wear/friction behaviour of FeB and FeB/h-BN coatings sprayed by atmospheric plasma spraying. Pract Metallogr 2007;44:355–71.
[25] Cartier M, McDonnell L, Cashell E. Friction of tungsten carbide-cobalt coatings obtained by means of plasma spraying. Surf Coating Technol 1991;48:241–8.
[26] Schwetzke R, Kreye H. Microstructure and properties of tungsten carbide coatings sprayed with various high-velocity oxygen fuel spray systems. J Therm Spray Technol 1999;8:433–9.
[27] Slvaramprasad G, Rao MV, Prasad D. Density and viscosity of ethanol þ 1, 2-dichloroethane, ethanol þ 1, 1, 1-trichloroethane, and ethanol þ 1, 1, 2, 2-tetrachloroethane binary mixtures. J Chem Eng Data 1990;35:122–4.
[28] Jääskeläinen H. Fuel property testing. Lubricity; 2008.
[29] Wagner J, Marotta E, Paradis I. Thermal modeling of engine components for temperature prediction and fluid flow regulation. SAE Technical Paper; 2001.
[30] Pickens D. Evaluating microscopic phenomena of lubricants at modified surfaces. Northwestern University; 2019.
[31] Qu J, Truhan JJ, Blau PJ. Investigation of the scuffing characteristics of candidate materials for heavy duty diesel fuel injectors. Tribol Int 2005;38:381–90.
[32] J.C. Russ, Fundamentals of energy dispersive X-ray analysis: butterworths monographs in materials, Butterworth-Heinemann2013.
[33] R. Baboian, Corrosion tests and standards: application and interpretation, ASTM international2005.